I J C T A, 9(32) 2016, pp. 295-311
© International Science Press

Design of Enhanced Field Oriented Flux Control Technique for Grid Connected DFIG Under Low Voltage Fault Ride Through

Polamraju. V.S.Sobhan[1], D.V.N. Ananth[2], G.V. Nagesh Kumar[3] and V Ravindranath Chowdary[4]

Abstract: In the next few decades, non-conventional wind resources add a great contribution to increased power demand. With major short circuit faults the system should regain to its normal state and ensure dynamic stability and provide better quality and reliable power, according to respective wind grid codes of the nation. Wind grid codes include behaviour under Low Voltage Ride Through (LVRT) and Reactive power provision at fault duration. This paper improves the LVRT and dynamic characteristics of the system with STATCOM during symmetrical and asymmetrical grid faults. The article will also show how Doubly Fed Induction Generator based wind turbine system will follow better grid code requirements with Enhanced Flux Oriented Control (EFOC) in Rotor Side Converter and also improves its dynamic behaviour with integrated three levels STATCOM controller. This can be achieved by minimizing DC offset currents to zero by controlling stator flux decay during transients. The stator d and q axis flux wave is circular during steady state and also deviate its shape and characteristics during transients. This feature is restored using EFOC technique and helps in maintaining a minimum voltage and current in rotor and stator circuit. This technique not only improves LVRT but also ensures a longer lifetime of the machine during major disturbances.

Keywords: DFIG; Field Oriented Control; LVRT; STATCOM

1. INTRODUCTION

With diminishing of primary fuels, renewable sources of energy like wind and solar power generation are getting significance due to eco-friendly nature and be made accessible from few kilowatts to megawatts rating. From many wind turbine based generators, DFIG is getting added significance due to maximum power extraction capability, variable speed generator running operation, and strong reactive power control, resist capability during low voltage and high voltage fault ride through, low cost of converters, work effectively during flickering and unbalanced types of load, deliver real power even generator speed reduces from super-synchronous speed to sub-synchronous speed mode for grid connected system. The reactive power control ability and competence enhancement is obtained with help of rotor side control (RSC). The RSC is rated between 25% to 35% range of generator rating permitting ±25% dissimilarity in rotor speed [1, 2]. Because of low power rating of RSC, the cost acquired on converter devices is low.

For a DFIG wind turbine system, both stator and also rotor will deliver power to the grid. The enhanced real and reactive power capability for DFIG system is given in [3, 4]. Under symmetrical 3-phase fault, stator of DFIG being sensitive, create a DC counterbalance part of flux which makes rotor voltage to forcibly pump additional current in the RSC [5], aggressive to the expectancy of power electronic devices. In the same way, asymmetric faults induce negative sequence flux components results in high currents with

1 Dept. of EEE, VFSTR University, Guntur, India, pvssobhan@gmail.cm
2 Dept. of EEE, VITAM College of engineering, Visakhapatnam, India, nagaananth@gmail.cm
3 Dept. of EEE, GITAM University, Visakhapatnam, India, drgvnk14@gmail.com
4 Dept. of EEE, GITAM University, Bengaluru, India.

real and reactive power and electromagnetic torque oscillations [6-8]. Hence controlling this over current, crowbar circuit [9] is generally used to avoid which disable DFIG and makes grid into more dangerous state. So, advanced vector control techniques etc., are used to improve fault current and voltages of stator and rotor and to damp power and electromagnetic torque oscillations. However above methods in RSC does not provide significant reduction in rotor over currents. The application of STATCOM for improved performance during transients for grid connected DFIG are given in [10-24].

For ensured flux trajectory and circular shape with controlled magnitude of flux, EFOC technique was developed. Under disturbance conditions, DC offset currents will be developed and due to this an exponential decay in flux takes place and converts to elliptical for single line to ground fault and a smaller circular trajectory with large swings and changing centre to circle is observed. Hence this method helps in decreasing DC offset current (DCOC) by changing stator synchronous frequency to grid reference synchronous frequency which further helps in restoring its shape and magnitude and makes system healthy and faster in action during transients. The further enhancement in dip in stator and rotor voltage and current waveform and improving rotor speed, a three level STATCOM was used. A comparison of EFOC based system without and with STATCOM was done and analysis without EFOC was done as text for references [21 and 22].

This paper presents LVRT behaviour using an Enhanced Flux Oriented Control (EFOC) to reduce over currents along with aid of three levels STATCOM connected through bidirectional switches to the dc link. The above objectives are achieved without sacrificing dynamic stability of DFIG system. The DFIG based EFOC with STATCOM helps in improving dynamic stability during symmetrical grid disturbances and to maintain voltage at dc link capacitor nearly constant.

2. MATHEMATCAL ANALYSIS OF RSC AND GSC CONVERTERS FOR GRID CONNECTED DFIG DURING STEADY STATE

The conventional field oriented control (FOC) scheme for DFIG is done in synchronously rotating frame to facilitate decoupled active and reactive power control and to enhance system performance due to transients by improving dynamic response. The DFIG equivalent circuit [10], [12] is as shown in Fig. 1, whose vector dynamics are independently shown in GSC and RSC control strategies.

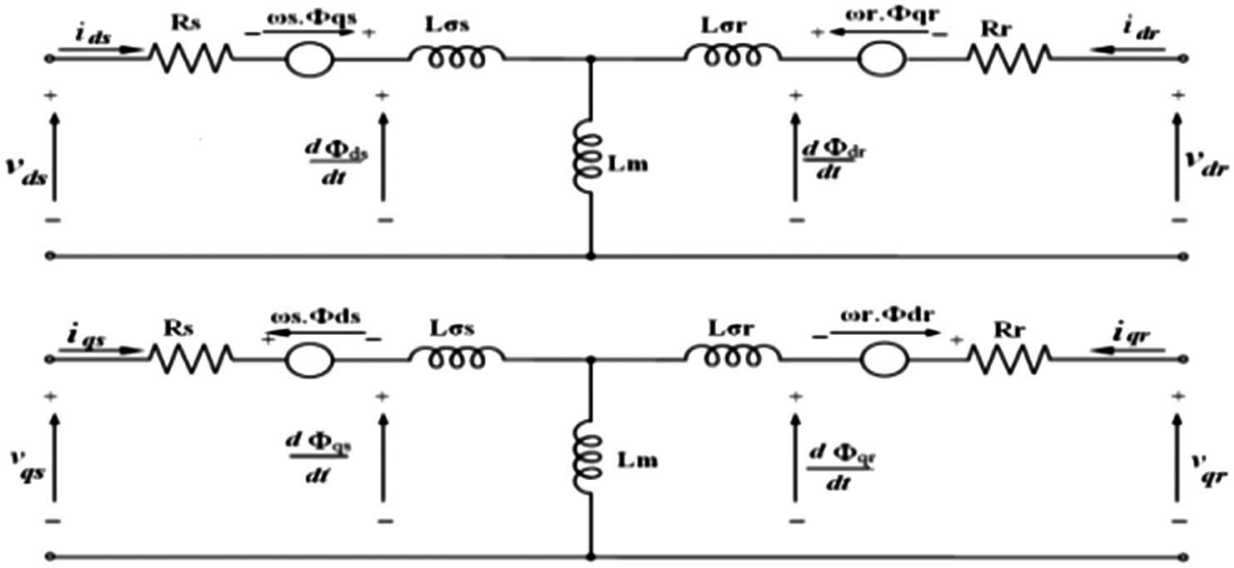

Fig. 1: Equivalent circuit of DFIG

2.1 Grid Side Converter Control

The proposed system is developed with EFOC strategy to provide rapid reactive power support to the grid through d and q axis components of grid voltage. The parks transformation is applied and sinusoidal PWM technique is used to feed gate pulses for Grid Side Converter (GSC). From Fig.2,

$$V_{ds} = i_{ds}R_s \quad -\omega_s \quad \phi_{qs} + \frac{d\phi_{ds}}{dt} \tag{1}$$

$$V_{qs} = i_{qs}R_s \quad -\omega_s \quad \phi_{ds} + \frac{d\phi_{qs}}{dt} \tag{2}$$

For a DFIG-grid system, the stator is directly connected to the grid, superior current regulation is obtained by adapting the above equations (1) and (2) to (3) and (4), whose control technique [4] is shown in Fig. 3.

$$V_{dg} = (i^*_{dg} \quad -i_{dg})R_s - \quad \omega_s \quad L_g i_{qg} + V_{ds} \tag{3}$$

$$V_{qg} = (i^*_{qg} \quad -i_{qg})R_s - \quad \omega_s \quad L_g i_{dg} \tag{4}$$

Where, $\frac{d\phi_{qs}}{dt} \cong 0$ specify non alignment of flux ϕ_{qs} with rotating stator quadrature flux. The suffix's' represents stator, where 'g' is for grid. The direct axis grid current depends on DC capacitor voltage and generates its reference i^*_{qg}. The exchange of reactive power between GSC and Point of Common Coupling (PCC) will depend on the grid d-axis current i^*_{qg} [8]. The decoupled components are compensated using cross couple grid terms $- \quad \omega_s \quad L_g i_{qg} \; V_{ds}$, and, $\omega_s \quad L_g i_{dg}$ which are added to the output of PI controller to circumvent coupling effects.

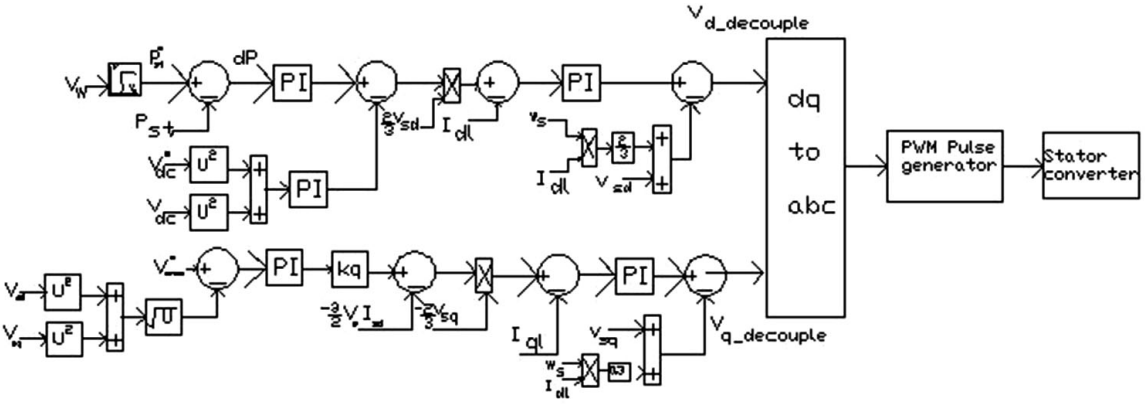

Fig. 2: GSC controller design for Grid connected DFIG

2.2 Rotor Side Converter Control

The Rotor Side Converter (RSC) controller helps in improving reactive power demand at grid in extracting maximum power from the machine for which the rotor is made to run at optimal speed. The optimal speed of the rotor is decided from machine real power and rotor speed characteristic curves from MPPT algorithm. The stator active and reactive power control is possible with the RSC controller strategy through i_{qr} and i_{dr} components controlling respectively. The rotor voltage in a stationary reference frame [11] is given by

$$V_r^s = V_{0r}^s + R_r i_r^s + \sigma \quad L_r \frac{di_r^s}{dt} - j\omega \quad i_r^s \tag{5a}$$

where, $\sigma = 1 - \frac{L_{sm}^2}{L_s L_r}$ and ω is the rotor speed, i_r^s is the rotor current in a stationary frame of reference, L_s, L_r, and L_m are stator, the rotor and mutual inductance parameters in Henry or in pu

$$V_{0r}^s = \frac{L_m}{L_s}\left(\frac{d}{dt} - j\omega_s\right) \quad \phi_s^s \tag{5b}$$

is the voltage induced in the stator flux with

$$\phi_s^s = L_s i_s^s + L_m i_s^s \tag{6}$$

$$\phi_r^s = L_r i_r^s + L_m i_r^s \tag{7}$$

The d and q axis rotor voltage equations (5a, b), (6) and (7) in the synchronous rotating reference frame are given by

$$V_{dr} = \frac{d\phi_{dr}}{dt} - (\omega_s - \omega) \quad \phi_{qr} + R_r \quad i_{dr} \tag{8}$$

$$V_{qr} = \frac{d\phi_{qr}}{dt} - (\omega_s - \omega) \quad \phi_{dr} + R_r \quad i_{qr} \tag{9}$$

The stator and rotor two axis fluxes are

$$\phi_{dr} = (L_{lr} + L_m) \quad i_{dr} + L_m \quad i_{ds} \tag{10}$$

$$\phi_{qr} = (L_{lr} + L_m) \quad i_{qr} + L_m \quad i_{qs} \tag{11}$$

$$\phi_{ds} = (L_{ls} + L_m) \quad i_{ds} + L_m \quad i_{dr} \tag{12}$$

$$\phi_{qs} = (L_{ls} + L_m) \quad i_{qs} + L_m \quad i_{qr} \tag{13}$$

where, $L_r = L_{lr} + L_m$, $L_s = L_m$, $\omega_r = \omega_s - \omega$

By substituting (10), (11), (12), (13) in (8), (9) and by rearranging the terms, then

$$V_{dr} = \left(R_r + \frac{dL_r'}{dt}\right) i_{dr} - s\omega_s L_r' \quad i_{qr} + \frac{L_m}{L_s} V_{ds} \tag{14}$$

$$V_{qr} = \left(R_r + \frac{dL_r'}{dt}\right) i_{qr} - s\omega_s L_r' \quad i_{dr} + \frac{L_m}{L_s}(V_{ds} - \omega\phi_{ds}) \tag{15}$$

Where ω is rotor speed, ω_s is synchronous speed.

Figure 3(i): RSC controller with EFOC technique design for Grid connected DFIG

The control circuit of RSC for enhancing performance for LVRT issues is shown in Fig. 3(i). The direct and quadrature axis (d and q axis) currents are used to control effectively flux decay during symmetrical or asymmetrical faults.

The overall block diagram of RSC is presented in Fig. 3(ii). The rotor speed is multiplied with pole numbers and is subtracted from angular grid synchronous frequency. Later integrated and given a 90o phase shift to get rotor slip injection frequency angles . At this slip frequency RSC converter injects current into the rotor circuit to control the rotor speed for optimum value and to control grid reactive power. The stator voltage magnitude is compared and controlled using PI or IMC controller to get q-axis current.

Similarly rotor actual speed and optimal speed reference are controlled using PI or IMC to get d-axis reference current. They are compared with an actual rotor *d* and *q* axis currents and controlled with tuned PI controllers to get the rotor injecting d and q axis voltages. The *d* and *q* voltages are converted into three axis abc voltage by using phase locked loop (PLL) with inverse parks transformation and is given to a PWM pulse generator for getting pulses to RSC converter.

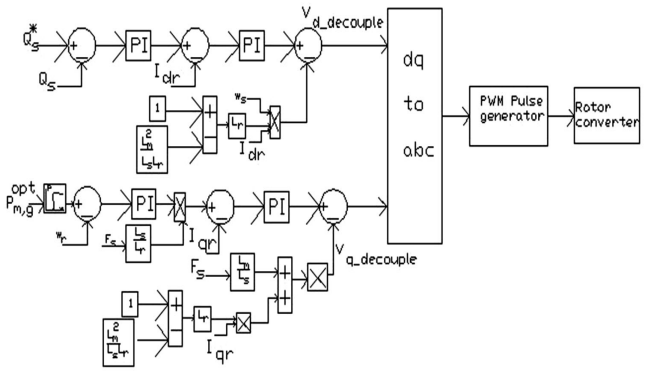

Figure 3(i): RSC controller with EFOC technique design for Grid connected DFIG

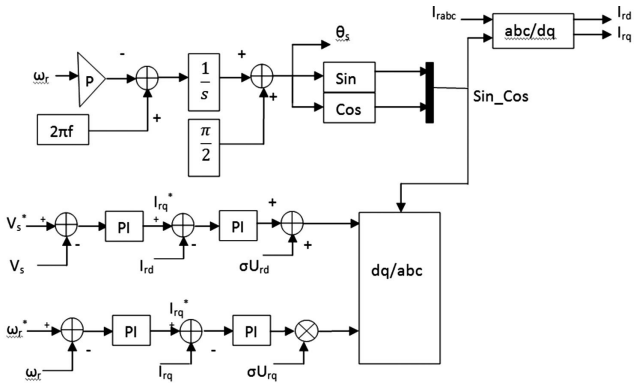

Fig. 3 (ii) Complete RSC controller design

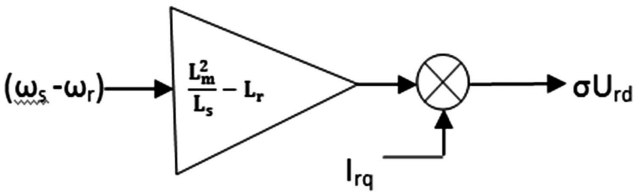

Fig. 3 (iii) Decoupled d-axis rotor voltage parameter

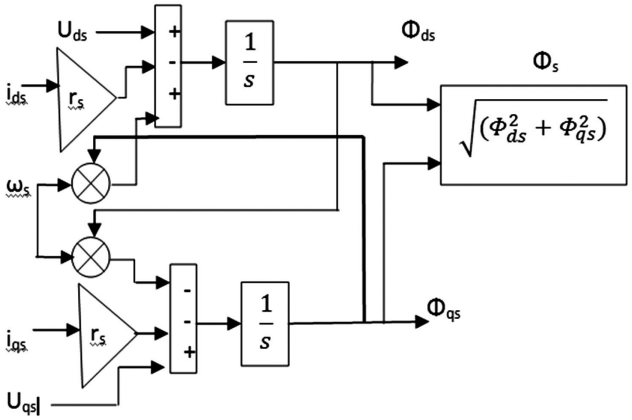

Fig. 3(iv) Block diagram representation of stator flux calculation

The *d*-axis decoupled voltage derivation block diagram is shown in Fig. 3 (iii). The d and q axis stator flux and stator flux magnitude derivation block diagram is shown in Fig. 3 (iv). The flux derivation technique helps in understanding the operation of DFIG during steady state and transient state.

3. MATHEMATCAL ANALYSIS OF RSC AND GSC CONVERTERS FOR GRID CONNECTED DFIG DURING TRANSIENT STATE

3.1 Three Phase Symmetrical Faults

The stator voltage will reach zero magnitude during severe three phase's symmetrical fault of very low impedance and stator flux ϕ_s gets reduced to zero magnitude. The decay in flux is not as rapid as in voltage

and delay is due to inertial time lag $\tau_s = \frac{L_s}{R_s}$ effecting the rotor induced Electromotive Force (EMF) V_{0r}. The flux during fault is given by

$$\phi^s_{sf} = \phi^s_s \quad e^{-t/\tau_s} \tag{16}$$

And $\frac{d\phi^s_{sf}}{dt}$ is negative, indicating its decay. By substituting (16) in (5b)

$$V^s_{0r} = -\frac{L_m}{L_s}\left(\frac{1}{\tau_s} + j\omega\right) \quad \phi^s_s \quad e^{-t/\tau_s} \tag{17}$$

Converting the above equation in the rotor reference frame and by neglecting $\frac{1}{\tau_s}$

$$V^s_{0r} = -\frac{L_m}{L_s}(j\omega) \quad \phi^s_s \quad e^{-j\omega t} \tag{18}$$

By substituting $\phi^s_s = \frac{V^s_s}{j\omega_s} \quad e^{-j\omega_s t}$ in (18)

$$V^s_{0r} = -\frac{L_m}{L_s}(1-s)V_s \tag{19}$$

$\left|V^s_{0r}\right|$ is proportional to $(1 - s)$

Converting equation (5a) into rotor reference frame

$$V^r_r = V^r_{0r} \quad e^{-j\omega t} + R_r i^r_r + \sigma \quad L_r \frac{di^r_r}{dt} \tag{20}$$

Thus rotor equivalent circuit derived from (20) is as shown in Fig. 4 [11].

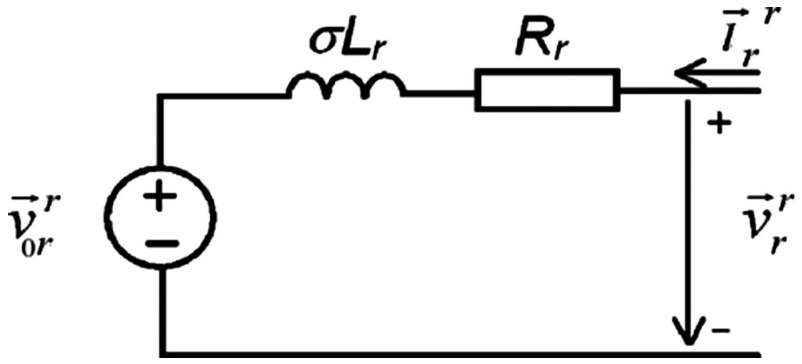

Fig. 4: The rotor equivalent circuit

A considerable decrease in pre-fault steady state voltage V^r_{0r} to certain fault voltage during a three phase fault was explained in above analytics. However, RSC converter is designed to meet V^r_r to match V^r_{0r} for rotor current control and the design has to be made for rating of only 35% of stator rated voltage.

The voltage dip during fault is adopted independently or in coordination by using two techniques.

During fault, at first instant, ϕ_s sdoes not fall instantly (16) as shown in the flux and voltage trajectories in Fig. 6. If the machine is running at super synchronous speed with slip (s) near to –0.2pu, during fault, rotor speed further increases based on the term$(1 - s)$ as given by (19). The above speed change is uncontrollable for a generator having higher electrical and mechanical inertia constants. In order to control the rotor current change, V_r^r has to be increased. Based on the first reason listed above, a voltage $V_{\phi s}$ has to be injected in the feed forward path for improving the rotor dip to reach to its near steady state value. Converting the equation (19) into a synchronous reference frame and by considering direct alignment of ϕ_s with we get,

$$V_{\phi s} = -\frac{L_m}{L_s}\omega\phi_{ds} \tag{21}$$

The second reason listed above is compensated by replacing $s\omega_s$ with $(\omega\phi_s - \omega)$ in cross coupling terms $s\omega_s L_r' \; i_{qr}$ and $s\omega_s L_r' \; i_{dr}$. The reduction in magnitude and frequency of flux ϕ_s, and alignment of flux with the stator voltage without rate of change in flux angle ϕ_s indicate *dc* offset component in flux. It is better observed in the voltage and flux trajectories shown in Fig. 5 for TLG and Fig.6 during SLG fault.

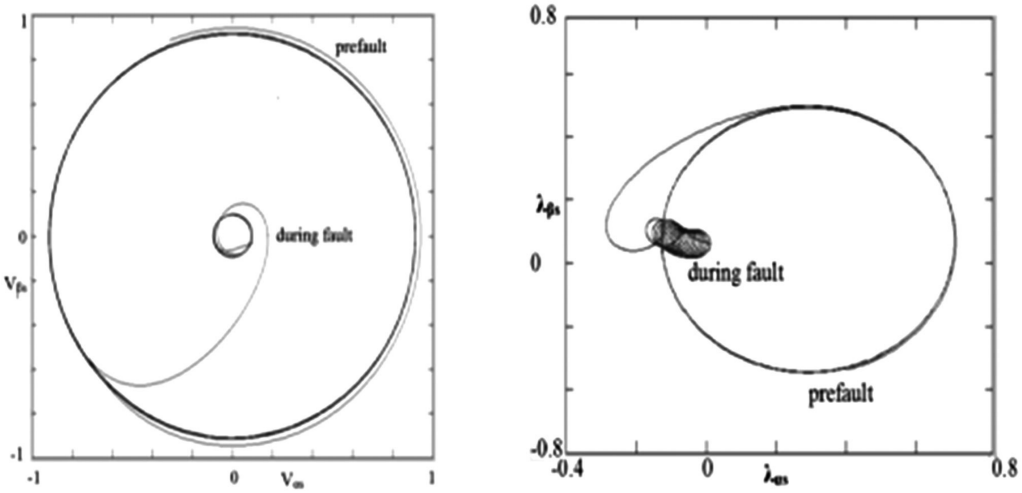

Fig. 5: Voltage and flux trajectories for symmetric (TLG) fault

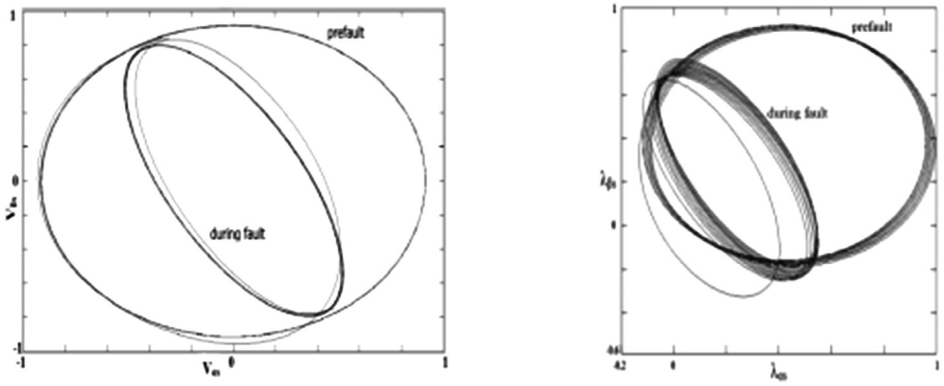

Fig. 6: Voltage and flux trajectories for asymmetric (single phase to ground) fault

$$\frac{d\theta_{\phi s}}{dt} = \omega_{\phi s} = 0 = \omega_f \tag{22}$$

where, ωf is the speed of stator flux during fault.

The voltage injection components (14, 15) and compensating components discussed above are estimated with enhanced flux oriented scheme whose flow chart is shown in Fig. 10 and the determined values are incorporated in RSC controller shown in Fig. 3.

3.2 Asymmetric Faults

The same control technique is employed for single phase to ground as well as two phase to ground faults. But due to presence of positive and negative sequence components, the rate of change in flux angle θ_s and magnitude change in flux is observed [4], given by

$$\frac{d\theta_{\phi s}}{dt} = \omega_{\phi s} = \frac{(V_{\beta s} \quad \phi_{\alpha s} - V_{\alpha s} \quad \phi_{\beta s})}{\phi_{\alpha s}^2 + \phi_{\beta s}^2} = \omega_f \tag{23}$$

The voltage and flux trajectories for a single phase to ground fault for the present system are shown in the Fig. 6.

4. DESIGN OF STATCOM AND ENHANCED FOC (EFOC) CONTROLLER FOR LVRT ISSUE FOR DFIG

The STATCOM controller is used for compensation of voltage at PCC and Enhanced Field Oriented Control technique (EFOC) is used for compensation of stator and rotor current of DFIG beyond the point of STATCOM controller. Compared to conventional FOC, flux decay rate is controlled by using this EFOC technique by controlling the DC offset current (DCOC) which is sub-transient DC component current of the generator. This controller technique further helps in maintaining the flux trajectory path of stator components not to go farther distance from centre of radius and reaching its pre-fault state even when the fault is not yet cleared. The techniques for STATCOM and EFOC are described below.

4.1 Voltage mitigation by STATCOM

The current injection and voltage to be compensated at PCC for safe operation and compensation are derived in this section with references from [20-23] and modified as per our work. The quadrature and direct axis voltages of STATCOM are given by

$$V_{qst} = M \quad V_{dc_{st}} \cos \quad (\theta_{st}) \tag{24}$$

$$V_{dst} = M \quad V_{dc_{st}} \sin \quad (\theta_{st}) \tag{25}$$

Where M is the modulation index of PWM θ_{st} is the load angle of STATCOM which is equal to $\theta_{PCC} + \alpha$, with θ_{PCC} and α are load angle at PCC and STATCOM power angle in degrees. $V_{dc_{st}}$ is the STATCOM DC voltage across the capacitor.

From literature compared to two levels STATCOM, three level STATCOM will work much better with good voltage and power factor compensation value, hence three level STATCOM was considered. The dip in the PCC voltage due to asymmetrical or symmetrical fault is compensated by STATCOM and the difference current compensation is given by

$$\frac{dV_{dc_{st}}}{dt} C_{st} = 2\pi f [I_{dc_{st}} - \frac{V_{dc_{st}}}{R_{st}}] \tag{26}$$

Where C_{st} is STATCOM voltage source converter (VSC) capacitor, $I_{dc_{st}}$ STATCOM injecting current and R_{st} is the voltage drop across switches, transformer and inductive filters between STATCOM and PCC terminals.

The current injected by three level STATCOM is given by

$$I_{dc_{st}} = M \quad I_{q_{st}} \cos \quad (\theta_{st}) + M \quad I_{d_{st}} \sin \quad (\theta_{st}) \tag{27}$$

4.2 EFOC control technique

The EFOC method of improving field flux oriented control technique helps in improving the performance of RSC controller of DFIG during fault conditions is described in Fig. 5. The DCOC observer does two actions the change in flux values of stationary frame stator references ($\phi_{\alpha s}$, $\phi_{\beta s}$) for tracking radius of trajectory and DCOC for offset change in stationary fluxes ($\phi_{dc\alpha s}$, $\phi_{dc\beta s}$) during fault conditions and controlling them The first action helps in not losing the trajectory from circle point and to reach its pre-fault state with same radius and centre of circle and hence improving same rate of flux compensation even during fault without losing stability. The second action helps in controlling and maintaining to nearly zero magnitude using DCOC technique.

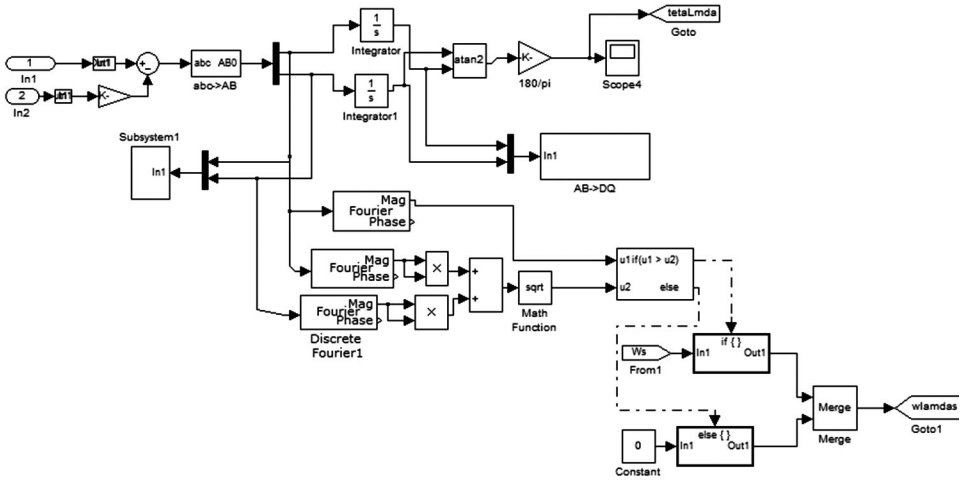

Fig. 7: EFOC control loop design with DCOC and rotor flux trajectory control

The outer loops are fast acting while inner two are slower for DFIG system. The difference in reference to actual two axis currents is controlled by well tuned PI controller for direct and quadrature axis rotor voltages. These outer PI controller output is manipulated with disturbance cross coupled voltages to achieve reference rotor voltage for pulse generation as shown in Fig. 3. The rotor pulses are generated at slip frequency rather than at fundamental for RSC.

The GSC controller design in MATLAB is shown in Fig. 2. For particular wind speed, reference or optimal mechanical power from turbine is estimated using characteristic lookup table. From equation (21), stator real power P_{stator} is measured and power error is difference between these two powers (dP) which has to be maintained to zero using PI controller. The PI output is then multiplied with real power constant (K_p) gives actual power to be controlled after disturbance.

In same way generally stator voltage (Vs* = 1) or reference reactive power (Qs* = 0), actual stator voltage Vs or reactive power Qs is decreased by PI controller and multiplied with reactive power constant (Kq) for actual reference reactive power recompense parameter. From equation (21), actual reactive power is designed and this difference and actual reactive power compensating terms and dividing with 2/3Vsq,

to get q-axis reference current (Iqref). The difference in Iqref and Iq is controlled by PI to get reference q-axis voltage. To improve transient response quickly and to minimize steady state error, decoupled q-axis voltage to be added . Both d and q axis voltage so obtained are converted to three axis 'abc' parameters with inverse Park's transformation and this voltage is given to PWM controller for grid side controller pulse generation.

The main purpose of rotor side controller (RSC) is to maintain desired generator speed and reactive power flow from rotor circuit, while grid side controller (GSC) is used to achieve nearly constant DC link voltage and to control bidirectional reactive power flow from GSC converter, stator and grid. This GSC is also capable in controlling real power from stator to achieve desired real power from generator stator.

5. RESULT ANALYSIS

The MATLAB/ SIMULINK based DFIG system for LVRT issue enhancement with EFOC technique and three levels STATCOM controller are described below under two cases with single phase and three phases to ground fault with fault resistance 0.001Ω at PCC during 1.2 to 1.6 seconds.

Case (a) Single Line to ground (SLG) fault without and with STATCOM

This type of fault mostly but severity on system disturbance is low. From Fig.8a, Fig.8b, it is observed that rotor voltage disturbance is low without or with STATCOM but rotor current increases from 0.2pu to nearly 0.48pu (per-unit) without STATCOM and 0.2pu to 0.3pu with STATCOM. Hence fault current entering to rotor is minimized using STATCOM. Compared to results from [21 or 22], with conventional FOC, EFOC will improve current and voltage drooping values during fault.

During SLG fault, stator of DFIG mostly gets affected due to severe fault inrush current entering into it. This makes stator voltage and current in general decreases drastically, but flux decay takes time which induces DC offset current in stator which damages stator and rotor windings if current further reaches rotor of DFIG. Hence this offset DC current is reduced by EFOC flux controller scheme explained in previous section. The rotor, stator and grid voltage drooping during SLG are shown in Fig.7a is without STATCOM and Fig.7 b with STATCOM. The voltage across STATCOM is shown in the bottom graph of Fig.7b. Similarly rotor, stator, grid current and STATCOM current without and with STATCOM for SLG fault are shown in Fig.8a and Fig.8b. It is observed that during SLG fault, the line with fault gets voltage decreased while other two healthy phases voltage increases from its nominal volues and further increase beyond particular value is controlled using STACTOM action.

The voltage across DC capacitor near the back-to-back converters of DFIG and rotor speed without and with STATCOM are shown in Fig. 9a and Fig.9b. It is observed that DC capacitor voltage ripples increases without STATCOM than with STATCOM, therefor RSC and GSC voltage changes much. With EFOC technique dc voltage at capacitor is maintained nearly constant, otherwise during fault, this dc voltage decreases during fault and increases like impulse voltage just after relieving of fault. Hence EFOC is much better technique than conventional FOC.

From the STATCOM voltage and current waveforms, during transient state, STATCOM current increases and that respective voltage changes in healthy and faulty lines are compensated. The spikes in the voltages during steady state helps in power factor control during steady state and these spikes are controlled by using inductor in series with the STATCOM phases which are generally used for PQ issues system. In our system, inductor was not used. The results when compared with [21 or 22], proposed control strategy is having less dip in machine parameters voltage. The tansient voltage and current are controlled effectively if STATCOM was incoroparated. However with STATCOM, current in fault line also be improved to its pre-fault state. It is to be noted that EFOC technique cant improve grid voltage or current and is done soley by STATCOM.

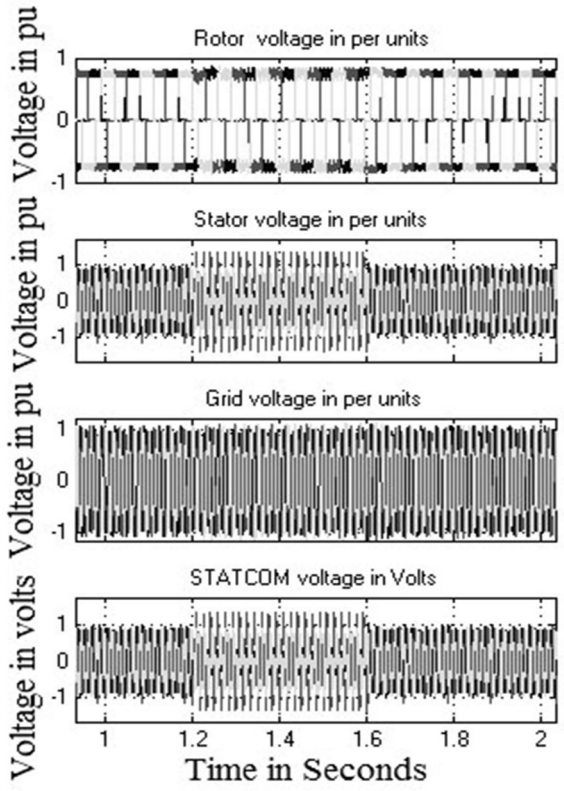

Fig. 7: (a)

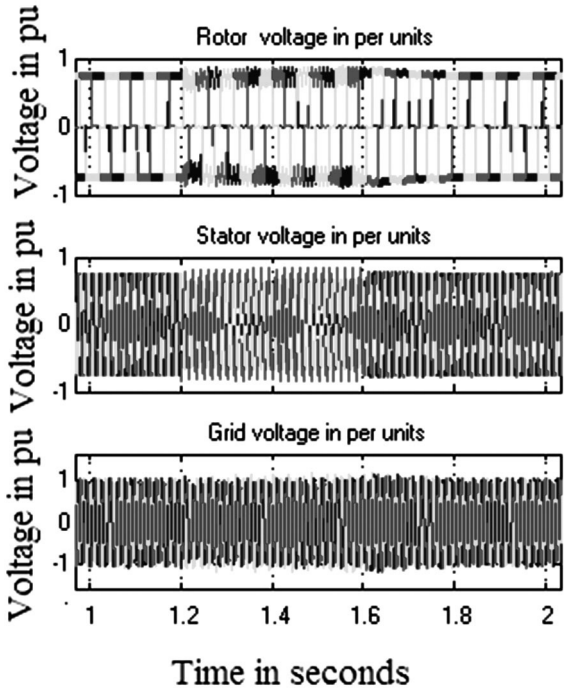

Fig. 7: (b)

Fig. 7: Rotor, Stator, Grid and STATCOM voltage a) without STATCOM and b) with STATCOM for SLG fault

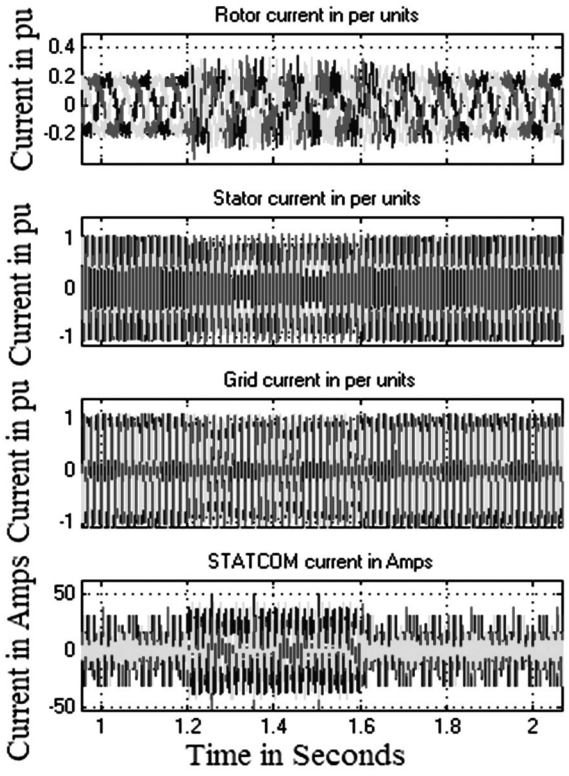

Fig. 8: (a)

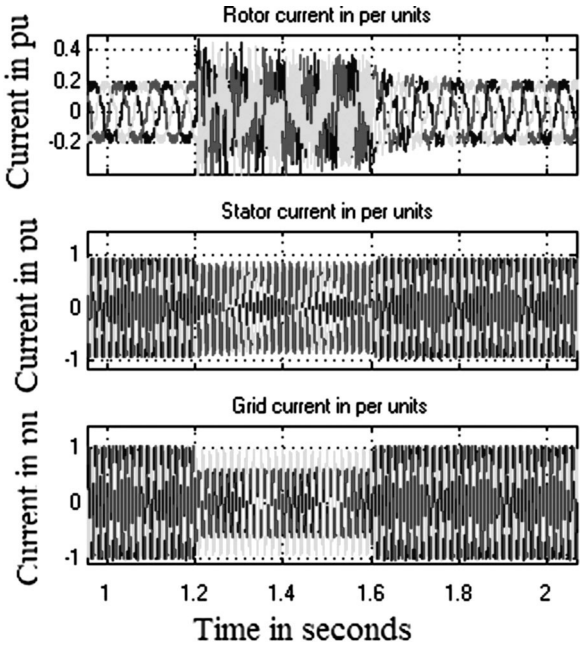

Fig. 8: (b)

Fig. 8: Rotor, Stator, Grid and STATCOM current (a) without STATCOM and (b) with STATCOM for SLG fault

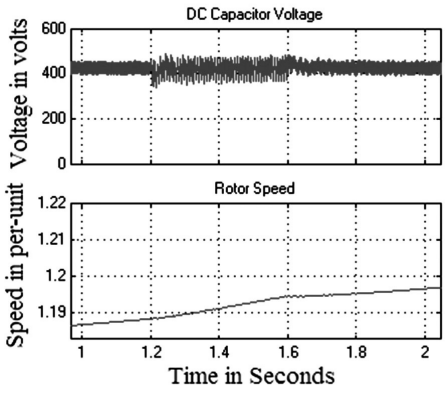

Fig. 9: (a)

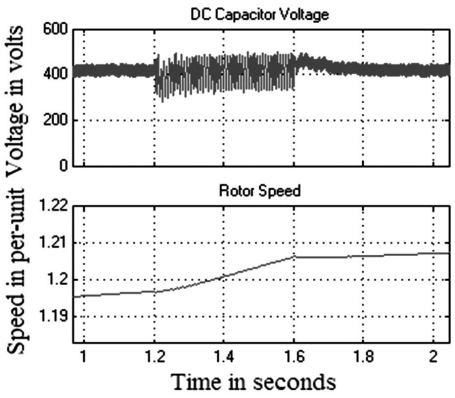

Fig. 9: (b)

Fig. 9: DC capacitor voltage of DFIG converters and rotor speed (a) without STATCOM and (b) with STATCOM for SLG fault

Case (b) Three line to ground (TLG) fault without and with STATCOM

A very severe symmetrical fault called TPG occurs at PCC during 1.2 to 1.6 seconds with same fault resistance of 0.001Ω. The rotor, stator, grid and STATCOM voltage waveforms without and with STATCOM are shown in Fig. 10a and Fig.10b. The rotor voltage decreases from 0.9pu reference to 0.45pu during fault and increased from 0.45pu to 2.2pu immediately after fault clearance without STATCOM. Without EFOC, the rotor voltage further decreased to 0.2pu and increased beyond 3.1pu which is not shown here can be observed in references [22, 21]. With EFOC and STATCOM controller, the drop in rotor voltage was minimized from 0.9pu to 0.85pu during fault and impulse rise immediately after fault is 1.04pu.

The rotor, stator, grid and STATCOM current waveforms without and with STATCOM are shown in Fig. 11a and Fig.11b. Since for a system without STATCOM, the STATCOM voltage and current will be zero. So, they are not shown in the waveforms. During the fault, fault current increases from 0.2pu to 0.49pu and decreased slowly during fault and post fault disturbances are also high without STATCOM. The rotor frequency during and just after fault change from slip frequency to higher value and reaches its normal state. With STATCOM, rotor current changes from 0.2pu to 0.38pu small change in rotor frequency and harmonics in rotor current waveform. STATCOM improves performance by minimizing rotor current oscillations.

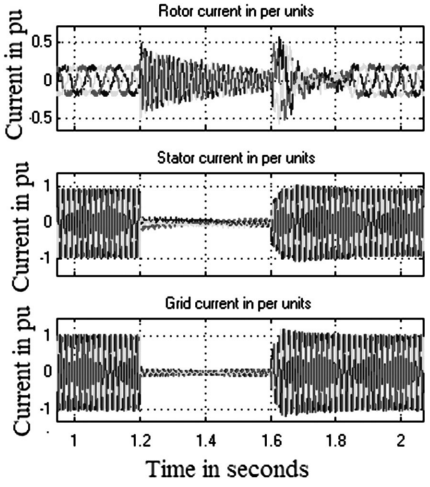

Fig 10: (a)

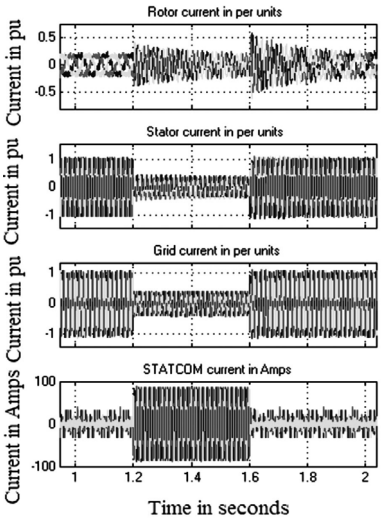

Fig. 10: (b)

Fig. 10: Rotor, Stator, Grid and STATCOM voltage a) without STATCOM and b) with STATCOM for TLG fault

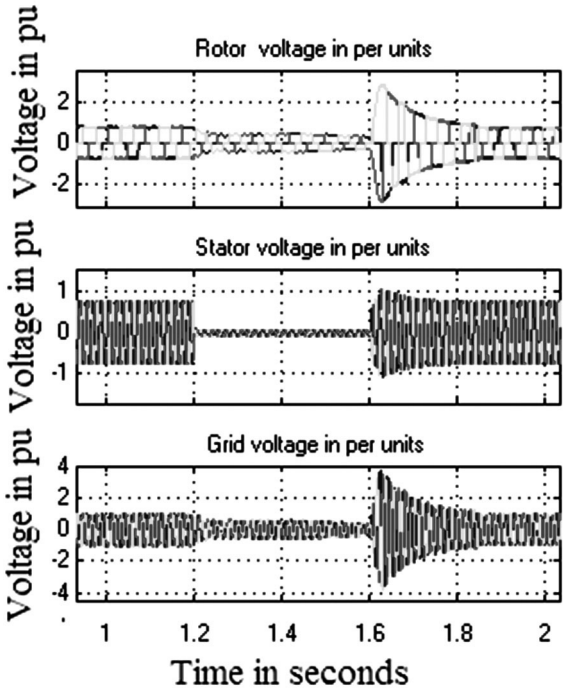

Fig. 11: (a)

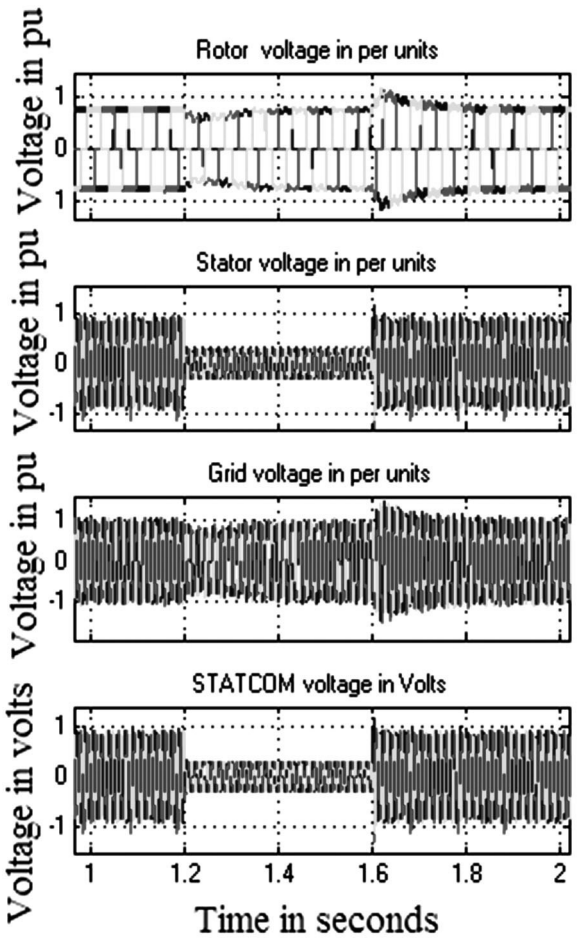

Fig. 11: (b)

Fig. 11: Rotor, Stator, Grid and STATCOM voltage a) without STATCOM and b) with STATCOM for TLG fault

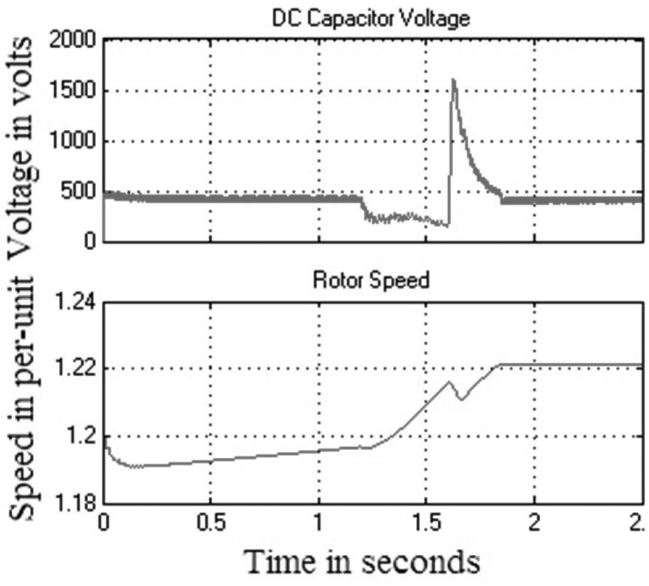

Fig. 12: (a)

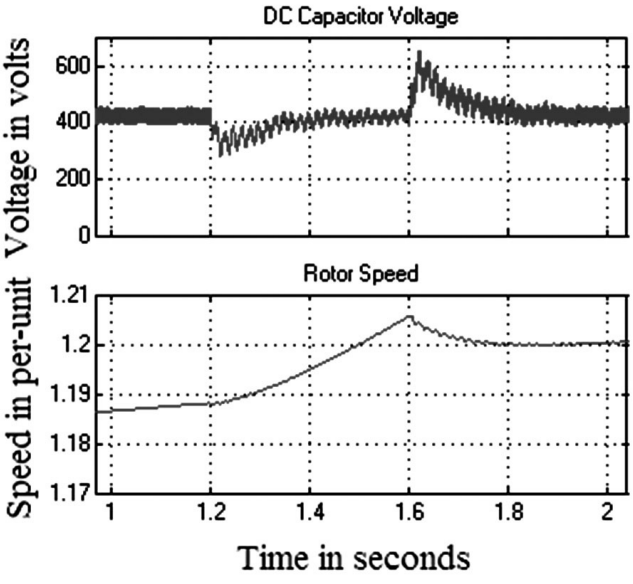

Fig. 12: (b)

Fig. 12: DC capacitor voltage of DFIG converters and rotor speed a) without STATCOM and b) with STATCOM for TLG fault

The drop in stator surge voltage during and just after fault without and with STATCOM, the fault voltage decreased from 1pu to 0.48pu and 3.75pu during fault and immediate fault relieving operation without STATCOM. The voltage value of stator was improved by STATCOM and helps in maintaing its during and post fault voltage value nearly constant. Also it is observed that during such severe fault, stator current decreased to very small value and is improved with STATCOM. With the help of EFOC, during this type of very severe fault with very low impedance value, stator current reaches its pre-fault immediately rather than slowly increasing. It was observed that with falut resistance value greater than 0.06Ω, compensation of stator current is 100% than without using EFOC. The grid voltage and current values without STATCOM was improved with STATCOM, with decrease in both voltage and current values lesser in later case.

The DC voltage across capacitor is shown in Fig.12a and Fig.12b without and with STATCOM. It is observed that DC capacitor voltage decreases from nearly 480V to 260V during fault and increases drastically to 1400V immediately after fault. Good GSC control scheme helps in maintaining DC voltage to certain value rather than becoming zero by absorbing fault current on grid side to reach to GSC and to charge capacitor. The rotor speed also maintained nearly constant with EFOC, otherwise this value reaches beyond 1.4pu speed of rotor and makes it to rotate at dangerous speed which may damage rotor windings of DFIG. But with STATCOM, decrease in DFIG back-to-back capacitor is low and also post fault DC current was only changed from 480V to 600V and reaches its 480V value in very small time period. Hence overall system behaviour was improved.

From the STATCOM voltage and current waveforms, it is observed that STATCOM voltage decreased and current level was increased so as to improve the injection current and load angle of it. During steady state operation, the STATCOM current was around 25 Amps and during fault it reaches to nearly 100 amps to compensate stator and rotor current and voltage and thereby grid terminal voltage and current values for enhanced stability and performance.

The DFIG WECS system is said to be in better operation when it provides good quality of power even when there are disturbances due to fluctuating wind speeds or grid faults. A good LVRT system will be ensued by improving dynamic stability by obeying respective country's wind grid codes. The proposed system offers LVRT capability as per NORDIAC grid code. The transient over current minimized in rotor circuit was advanced using EFOC technique and STATCOM controller avoiding crowbar application which has drawback of throwing grid into more vulnerable condition by challenging reactive power.

The dynamic behaviour of overall system was improved by limiting fault and post fault transient currents entering in generator system by making lethargic system to reach its steady value at an improved rate. Hence good quality and reliable power with the aid of EFOC and STATCOM will be achievable.

6. CONCLUSION

The proposed technique shows the effectiveness of EFOC technique and STATCOM controller and a comparison was made with and without STATCOM in all aspects of rotor, stator, grid and STATCOM voltages, current, dc capacitor voltage and rotor speed during and after three phase symmetrical and asymmetrical faults. The effect of SLG fault with EFOC does not cause much disturbance without or with STATCOM than in comparison with conventional FOC technique. Here both voltage of both stator and rotor remained constant while current there is some change in current in these. However grid voltage and current got disturbed due to the same fault proves the efficacy of EFOC technique. There are certain ripples in DC voltage at capacitor at back-to-back points of DFIG converters and not getting drooped to lower voltage value in comparing with general FOC. With STATCOM, ripples in DC voltage got much lesser. Rotor speed is nearly constant during and after transient recovery operation.

A very severe fault with very low resistance value occurs at PCC, makes stator, rotor and grid voltage and current to a low value during fault. The rotor current is not getting zero value in ampere per unit and got much better performance with incorporation of STATCOM into the circuit. For such faults, STATCOM is better option for much faster recovery of machine parameters and improved reliability and stability. A fault with little higher resistance can make rotor voltage and current value not to decrease much and can perform much better than in [11, 23, 24].

References

1. Ananth, D.V.N., Kumar, G.V.N., Gayathri, T, "Analysis and design of enhanced real and reactive power control schemes for grid connected Doubly Fed Induction Generator", Proc. IEEE INDICON, 2013 , pp: 1 – 6.
2. Gayathri, T, Ananth, D.V.N,Kumar,G.V.N, Sivanagaraju G, "Enhancement in Dynamic and LVRT Behaviour of an EFOC Controlled DFIG with Integrated Battery Energy Storage System", Proc IEEE INDICON,2013 , pp:1 – 6.
3. Asha Rani, M.A. ; Nagamani, C. ; Ilango, G.S. ; Karthikeyan, A., "An Effective Reference Generation Scheme for DFIG With Unbalanced Grid Voltage", IEEE Tran. Sust. Ener. Vol 5 , Is: 3, 2014 pp:1010 - 1018
4. Mokryani, G. ; Siano, P. ; Piccolo, A. ; Zhe Chen, "Improving Fault Ride-Through Capability of Variable Speed Wind Turbines in Distribution Networks", Systems Journal, Vol. 7, Is:4, pp:713-722
5. Jiaqi Liang, Wei Qiao, Harley. R.G, "Feed-Forward Transient Current Control for Low-Voltage Ride-Through Enhancement of DFIG Wind Turbines," IEEE Trans. Energy Conversion, vol.25, no.3, pp. 836-843, Sept 2010.
6. Lixin Ma, Yiwen Zheng, Heran Ma, "Research and simulation of double-fed wind power generation rotor side control technology," Electrical and Control Engineering (ICECE), 2011 International Conference, pp. 2472-2475, Sept 2011.
7. Sylvain .L. S, "Voltage Oriented Control of Three-Phase Boost PWM Converters," M.S. thesis, Dept. Elec. Power Eng., Chalmers Univ. of Tech., Goteborg, Sweden, 2010.
8. Bijaya Pokharel, "Modeling, Control and Analysis of a Doubly Fed Induction Generator Based Wind Turbine System with Voltage Regulation," M.S. thesis, Dept. Elec. Eng., Tennessee Tech. Univ., Tennessee, Dec 2011.
9. Abdou, A.F. ; Abu-Siada, A. ; Pota, H.R., "Application of STATCOM to improve the LVRT of DFIG during RSC fire-through fault", Proc. IEEE AUPEC, 2012 22nd Australasian , 2012 , pp: 1 – 6.
10. Beheshtaein, S., "Optimal hysteresis based DPC strategy for STATCOM to augment LVRT capability of a DFIG using a new dynamic references method", Proc. IEEE ISIE, 2014 , pp: 612 – 619.
11. Juan Shi ; Furness, I. ; Kalam, A. ; Peng Shi, "On low voltage ride-through and stability of wind energy conversion systems with FACTS devices", Proc. IEEE AUPEC, 2013 , pp: 1 – 6.
12. Mohaghegh Montazeri, M. ; Xu, David ; Bo Yuwen, "Improved Low Voltage Ride Thorough capability of wind farm using STATCOM", Proc. IEEE IEMDC, 2011 , pp: 813 – 818.
13. Lopez. J, Sanchis. P, Roboam. X, Marroyo. L, "Dynamic Behavior of the Doubly Fed Induction Generator During Three-Phase Voltage Dips," IEEE Trans. Energy Conversion, vol. 22, pp. 709-717, Sept. 2007.
14. Okedu.K.E, Muyeen.S. M,Takahashi. R, Tamura J, "Comparative study of wind farm stabilization using variable speed generator and FACTS device," GCC Conference and Exhibition (GCC), 2011 IEEE , pp. 569-572, Feb 2011.
15. Johan Morren, Sjoerd W. H. de Haan, "Ride through of Wind Turbines with Doubly-Fed Induction Generator During a Voltage Dip," IEEE Trans. Energy Conversion, vol. 20, pp. 435-441, June 2005.
16. Seman. S, Niiranen. J, Arkkio. A, "Ride-Through Analysis of Doubly Fed Induction Wind-Power Generator Under Unsymmetrical Network Disturbance," IEEE Trans. Power Systems, vol. 21, pp.1782-1789, Nov 2006.
17. Erlich. I, Wrede. H, Feltes. C, "Dynamic Behavior of DFIG-Based Wind Turbines during Grid Faults," Power Conversion Conference - Nagoya, 2007. PCC '07, pp. 1195-1200, April 2007.
18. Pannell. G, Zahawi. B, Atkinson. D. J, Missailidis. P, "Evaluation of the Performance of a DC-Link Brake Chopper as a DFIG Low-Voltage Fault-Ride-Through Device," IEEE Trans. Energy Conversion, pp. 1-8, May 2013.
19. Pal. B. C. Coonick. A. H. Macdonald, Donald. C, "Robust Damping Controller Design In Power Systems With Superconducting Magnetic Energy Storage Devices," IEEE Trans. Power Systems, vol. 15, pp. 320-325, Feb 2000.
20. Serhiy V. Bozhko, R.B.Gimenez,R.Li, Jon C. Clare, G. M. Asher, "Control of Offshore DFIG-Based Wind Farm Grid With Line-Commutated HVDC Connection", IEEE Tran. Ene. Conv., Vol. 22, No. 1, Mar. 2007, pp: 71-78.

21. Serhiy Bozhko, Greg Asher, Risheng Li, Jon Clare, Liangzhong Yao, "Large Offshore DFIG-Based Wind Farm With Line-Commutated HVDC Connection to the Main Grid: Engineering Studies", IEEE TRAN. ENE. CONV., VOL. 23, NO. 1, MAR. 2008, pp: 119-127.

22. Wei Qiao, Ronald G. Harley, G.K. Venayagamoorthy, "Coordinated Reactive Power Control of a Large Wind Farm and a STATCOM Using Heuristic", IEEE TRAN. ENE. CONV., VOL. 24, NO. 2, Jun. 2009, pp: 493-503.

23. Wei Qiao, Ganesh Kumar Venayagamoorthy, Ronald G. Harley, "Real-Time Implementation of a STATCOM on a Wind Farm Equipped With Doubly Fed Induction Generators", IEEE TRAN.IND. APP., VOL. 45, NO. 1, JAN./FEB. 2009, pp: 98-107.

24. Li Wang, Chia-Tien Hsiung, "Dynamic Stability Improvement of an Integrated Grid-Connected Offshore Wind Farm and Marine-Current Farm Using a STATCOM", IEEE TRAN. POW. SYS. VOL. 26, NO. 2, MAY 2011, pp: 690-698.

Appendix

The parameters of DFIG used in simulation are, Rated Power = 1.5MW, Rated Voltage = 690V, Stator Resistance R_s = 0.0049pu, rotor Resistance R_r□ = 0.0049pu, Stator Leakage Inductance L_{ls} = 0.093pu, Rotor Leakage inductance L_{lr}^{1} = 0.1pu, Inertia constant = 4.54pu, Number of poles = 4, Mutual Inductance Lm = 3.39 pu, DC link Voltage = 415V, Dc link capacitance = 0.2F, Wind speed = 14 m/sec. Grid Voltage = 25 KV, Grid frequency = 60 Hz Grid side Filter: R_{fg} = 0.3Ω, L_{fg} = 0.6nH Rotor side filter: R_{fr} = 0.3mΩ, L_{fr} = 0.6nH STATCOM: capacitance= 20,000UF, transformer-690/440V, 50kVA rating.